Response Properties of a Sensory

Hair Excised from Venus's Flytrap

R. M. BENOLKEN and S. L. JACOBSON

From the University of Texas Graduate School of Biomedical Sciences, Texas Medical Center, Houston, Texas 77025, and the Department of Biology, Carleton University, Ottawa 1, Canada

ABSTRACT Multicellular sensory hairs were excised from the leaf of Venus's flytrap, and the sensory cells were identified by a destructive dissection technique. The sensory layer includes a radially symmetrical rosette of 20–30 apparently identical cells, and the sensory cells are organized in a plane normal to the long axis of the sensory hair. The sensory cells were probed with intracellular glass electrodes. The resting membrane potential was about -80 mv, and the response to a mechanical stimulus consisted of a graded response and an "action potential." The action potential appears to be similar to the action potential which propagates over the surface of the leaf. In the absence of stimulation, the upper and lower membranes of a single sensory cell behave in an electrically symmetrical fashion. Upon stimulation, however, the upper and lower membranes become electrically asymmetrical. Limiting values for the response asymmetry were calculated on the hypothesis of an electrical model consistent with the histology of the sensory cells.

INTRODUCTION

Venus's flytrap, *Dionaea muscipula*, is a plant which traps and digests insects. The preying structure consists of a bilaterally symmetrical leaf or trap. Before stimulation, the two lobes of the leaf are separated by an angle of about 60 degrees. When stimulated by a prey, the bilobed leaf closes along a line defined by the midrib which separates the two lobes of the leaf. Closure occurs in two phases. In the initial quick phase, the leaf closes so that the marginal hairs interdigitate and trap the prey within about 100 msec of the last stimulus. A slower phase follows in which the two lobes appear to contract very tightly about the prey—so tightly, in fact, that the outline of the prey is obvious when looking at the trap. Thereafter the trap remains closed for a period of about 2 wk and the prey is digested by secretions from glands located on the surface of the trap. The trap reopens at the end of the 2-wk period to expose the chitinous remains of the insect. The procedure is different if the trap closes without catching its prey; then the trap remains closed for only a matter of hours before reopening.

64

Trap closure is a precisely controlled process. The process is initiated when the prey deflects sensory hairs located on the trap. Usually each trap has six sensory hairs, three on each lobe. A minimum requirement for closure is that one sensory hair be stimulated twice or that each of two hairs be stimulated once. The time sequence in which the stimuli are delivered is crucial for closure. Two stimuli are sufficient for closure if both occur within a time interval of approximately 30 sec. If the stimuli are separated in time by much more than 30 sec, three successive stimuli may be required before closure is initiated. This time series may be programmed for a period of hours. Brown (1916) reported that a series of 18 stimuli separated by intervals of 18 min elicited closure; apparently some effect of the stimuli was "remembered" for more than 5 hr.

The sensory hair is a multicellular structure about 200 μ in diameter at the base and about 2 mm in length. The distal woody structure or "lever" of the hair is not required for closure since stimulation of the proximal "podium" region alone is sufficient to elicit closure (Brown and Sharp, 1910). An action potential propagates over the leaf of a trap when a sensory hair is deflected or when trap tissue is stimulated electrically (Burdon-Sanderson, 1873), and propagated action potentials, at least two in number, always precede closure (DiPalma et al., 1961). The propagated action potential has been recorded with intracellular electrodes (Sibaoka, 1966).

A graded electrical response to stimulation is observed when one external electrode is placed on the cut tip of a hair and a second is placed on the leaf. A threshold for occurrence of an action potential is defined for a given magnitude of the graded response, and the properties of the graded response are a function of both the amplitude and waveshape of the mechanical stimulus (Jacobson, 1965). The graded response originates in the sensory hair, since it can be recorded from a hair which has been excised from a trap (Benolken and Jacobson, 1967).

The sensory input to the program which controls closure of a trap is shown below

Adequate	Threshold	Action potential
mechanical →	graded →	propagated over
stimulus	response	the trap surface

where at least two complete sequences of this type are required as a minimum condition for closure. The model and the data from which it was derived do not answer the questions (a) where or (b) how the graded response is coupled to the all-or-none propagated action potential, (c) whether the complicated waveshape of the sensory response recorded with gross extracellular electrodes is the result of a complicated single unit response or whether it results from an asynchronous summation of uncomplicated unit responses, or (d) how the

stimulus memory system is programmed to operate on two or more input sequences. The data which follow probably provide an answer to the first three questions. The fourth question regarding stimulus memory remains as elusive as ever. However, the resting membrane potential of the sensory cell does not appear to act as an accumulator in the process.

MATERIALS AND METHODS

Sensory hairs were freshly excised from healthy plants of *Dionaea muscipula*. The plants were raised from 10-year or older bulbs supplied by Insectivorous Botanical Garden, Wilmington, N. C. The proximal end of an excised hair was held by capillarity on a moist cotton brush and inserted into one hole of a 60-mesh, stainless steel, electron microscope grid (referred to hereafter as an EM grid) as shown in Fig. 1. The upper and lower preparation chambers were electrically isolated by a layer of beeswax which sealed and insulated the EM grid openings. The beeswax also provided good mechanical support for the hair. The upper and lower chambers were filled with 1 mM KCl adjusted to pH 6.5 with 1 mM Tris and HCl for the destructive dissection experiments. A perfusion fluid was used for the intracellular recordings, and the ionic composition of the perfusion fluid was derived from a microchemical analysis of the extracellular sap which was extracted from the plant by Jacobson (1968). The perfusion fluid had the following composition

	mM
K	1.0
Na	9.0
Ca	2.0
Mg	4.3
Cl	14.0
SO$_4$	4.3
Tris-maleate buffer	4.5 at pH 6.5

Reference Ag-AgCl electrodes could be switched to make contact with either the upper or lower chamber; i.e., on either side of the insulated EM grid. The recording electrode was an Ag-AgCl cotton wick for the destructive dissection experiments. The intracellular electrodes consisted of glass micropipettes filled with 0.1 M KCl which formed a salt bridge between the preparation and perfusion fluid in contact with an Ag-AgCl electrode. The DC impedance of the micropipettes ranged from 500 to 1200 megohms. The Ag-AgCl electrodes were connected to either a MacNichol and Wagner preamplifier (1954) or to one of our own design. Responses were monitored in the usual way with an oscilloscope and pen writers.

Mechanical stimuli were controlled with a Beckman-Offner model 506 pen-writing galvanometer driven by a model 473 power amplifier. The unloaded frequency response of the mechanical system was ±1 db or better from DC to 1 kHz for the small deflections required here. The position of the mechanical driver could be controlled with a precision of a few microns. Since the sensory hair was excised from the plant for these experiments, it could not be stimulated by bending the hair on the leaf. Consequently a stationary backup tool was placed against one side of the sensory

region, and a force was exerted by the galvanometer driver on the opposite side of the hair. As far as the extracellular response was concerned, no significant qualitative differences were observed for these stimuli when compared to the usual bending stimuli produced by deflecting the hair before it was excised from the leaf.

The position of the stimulus driver was monitored for the destructive dissection experiments, while both position and force were monitored for the intracellular experiments. Position was monitored optically with a differential pair of photodetectors of our design. Differences in position could be measured with a precision of a few
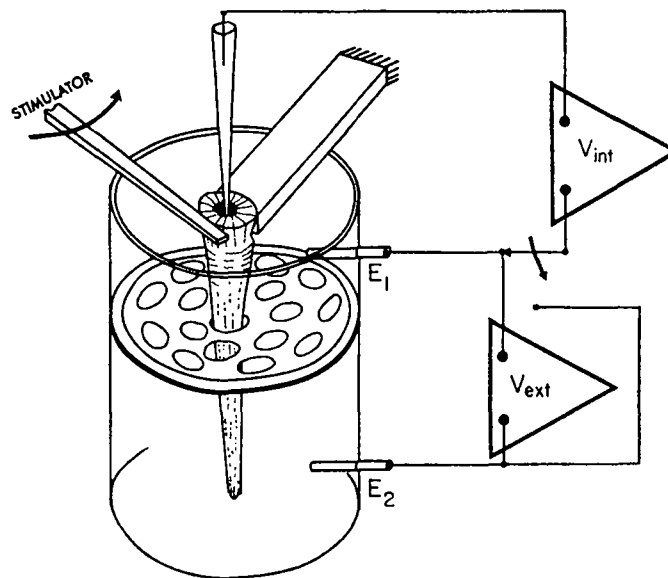

Figure 1. Excised hair preparation. An excised sensory hair was supported by an electron microscope grid, and the grid was insulated to isolate the upper (podium) chamber from the lower (lever) chamber. E_1 defines the potential of an electrode in contact with the bathing solution in the upper chamber, and E_2 defines the potential of an electrode in contact with the bathing solution in the lower chamber. The extracellular potential difference is defined by $V_{ext} = (E_2 - E_1)$. V_{int} is the potential difference measured between a micropipette inside a cell and an external reference electrode. The reference location could be switched to E_1 or to E_2.

microns. Stimulus force was measured as a linear function of the difference between the galvanometer driving voltage and the output voltage of the position sensor. The position of the stimulator, measured optically, was a linear function of the galvanometer driving voltage when the driver was unrestrained. The difference between where the driver position would have been if unrestrained and its actual position provided a measure of the resistive force. Newton's third law predicts that the resistive force so measured should be equal in magnitude and opposite in direction to the driving force of the stimulator. After calibration with measured resistive forces, the difference between the galvanometer driving voltage and the output of the position sensor pro-

vided a linear force measure to a precision of a few milligrams over the experimental range reported here.

RESULTS

Part 1. Identification of the Sensory Cells

A sensory hair was excised from a leaf and mounted as shown in Fig. 1. A high-impedance waxy cuticle covers the distal lever portion of the hair, and the tip of the lever was cut off in order to reduce the access impedance to the sensory region. A wick electrode made contact with the surface of the podium exposed in the upper chamber. The hair was stimulated by mechanical compression, the response was recorded, and then a slice of tissue one or two cell layers thick was cut from the upper end of the hair. The tissue slice was fixed in buffered glutaraldehyde and subsequently embedded in araldite. This process was repeated at 10-min intervals until the response vanished, usually at a well-defined endpoint. When the response vanished, it was assumed that the sensory cells were contained in the preceding tissue slice.

The results of a typical experiment are shown in Fig. 2. The upper trace monitored the position of the stimulus driver, the second trace monitored the response to stimulation, longitudinal tissue sections are shown below the corresponding response records, and the tissue slices from which the sections were derived are shown at the bottom of the figure. The response remained relatively uniform until after section 3 was removed in this experimental run, and it vanished after section 3 was removed from the sensory hair. The histology indicated that section 3 was about one cell layer thick, and the only intact cells in the section were those that occur at the level of indentation of the sensory hair. This result was observed consistently: When the "indented" cell layer was destroyed, the response vanished. A cross-section and a longitudinal section of the hair at the level of the indented cells are shown in Fig. 3. This layer includes 20–30 elongated epidermal cells arranged in a radially symmetrical fashion. These cells are characterized by an indentation of their outer walls. The indentations are in register and produce an indented band around the entire hair at this level. This provided a convenient landmark for identifying the level of the sensory cell layer in an intact hair.

Occasionally in an experimental run similar to that shown in Fig. 2, the response was substantially reduced after one slice and abolished after the next slice. Examination of the first slice usually showed that it was cut somewhat obliquely to the long axis of the hair and that some of the indented cells on one side of the rosette were intact. Although these data are few and inconclusive, they seem to argue against the possibility that one or only a few unique cells contribute to the extracellular sensory response. The extracellular response appears to be the result of a summation of outputs from apparently similar sensory cells.
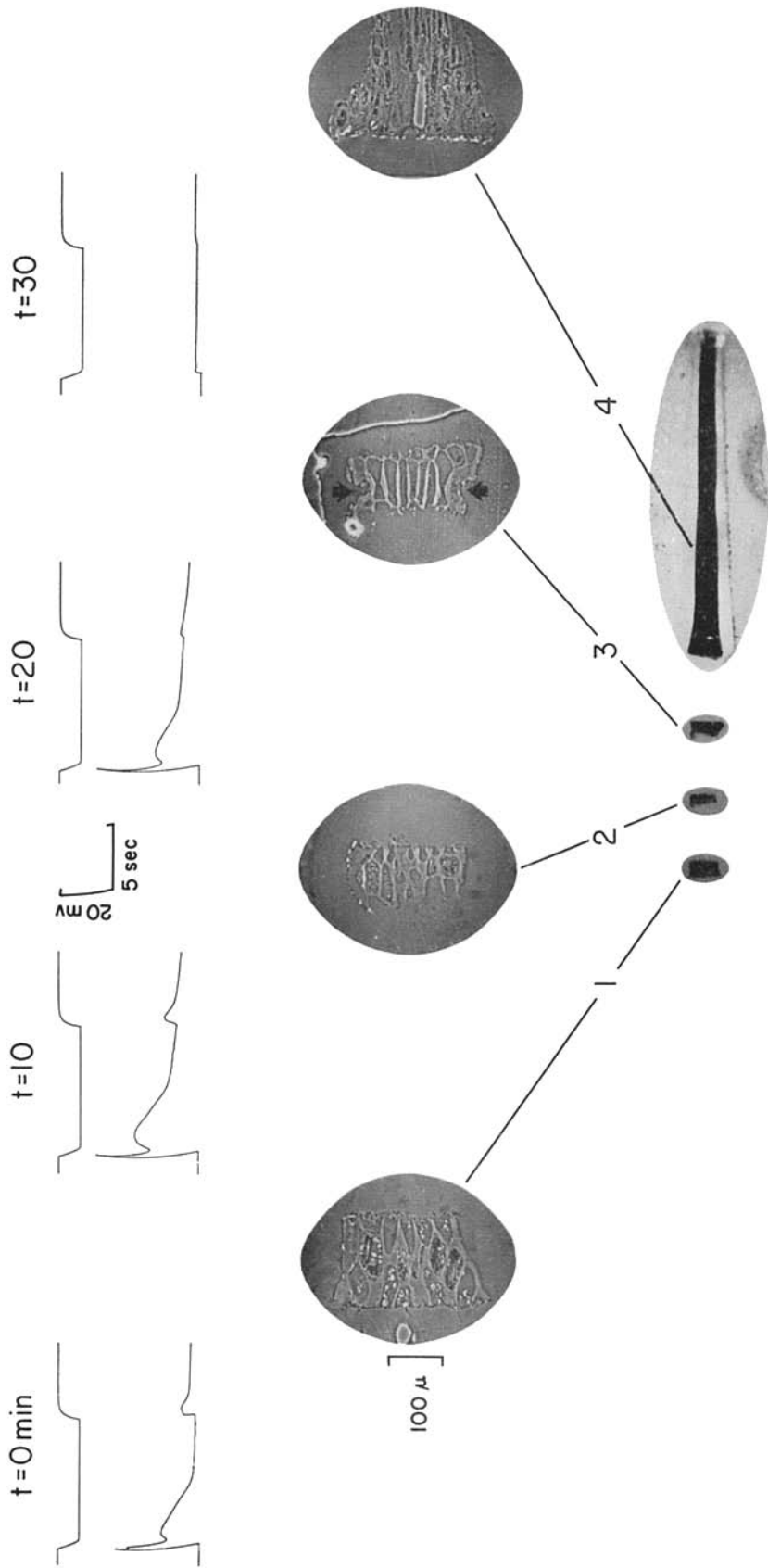
FIGURE 2. Typical result of destructive dissection. Stimulus displacement was recorded on the upper trace with maximum amplitude approximately 25 μ. V_{ext} was recorded on the second trace with positive upward. The amplitude calibration applies to the second trace. The radius of curvature of the curvilinear recording system is indicated on the amplitude calibration. The time calibration applies to both recording traces. Longitudinal sections of tissue slices are shown below the corresponding response records. Embedded tissue slices, from which the longitudinal sections were derived, are shown at the bottom of the figure. Arrows in section 3 indicate the indentations which are characteristic of the sensory layer.
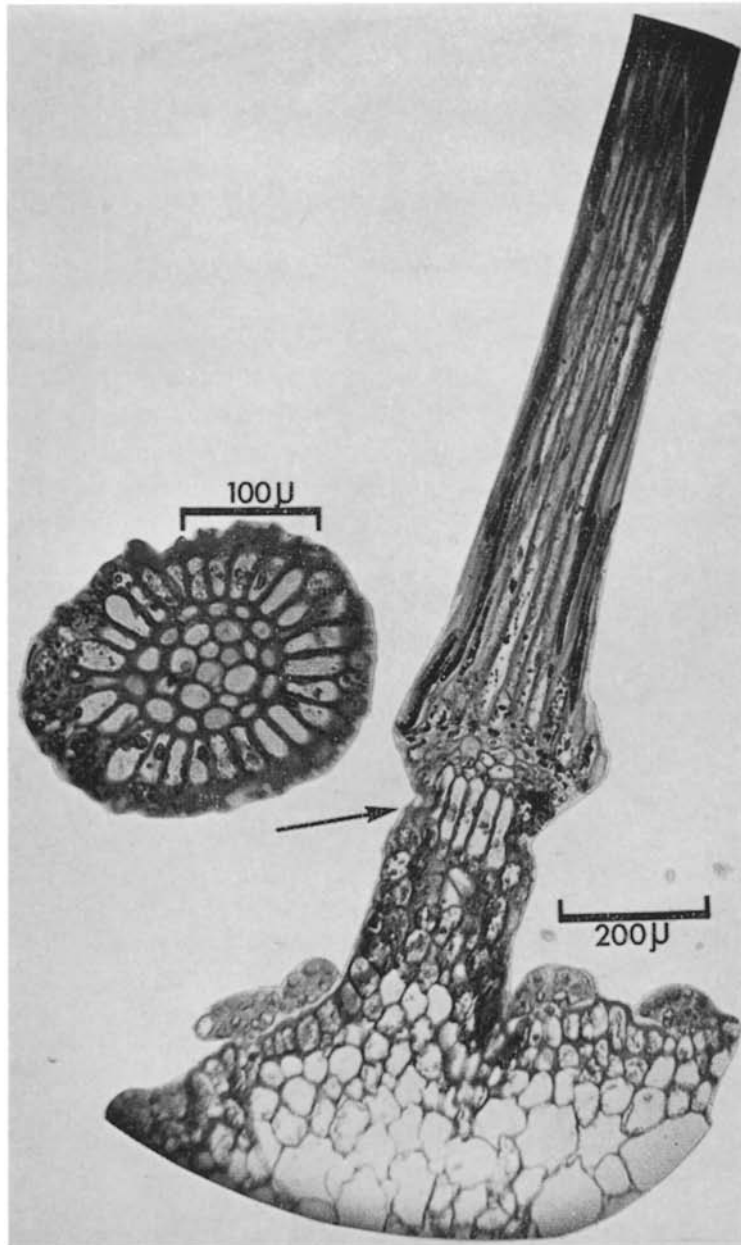
FIGURE 3.   Cross-section and longitudinal section of a sensory hair. The cross-section at the left was selected from the indented level of a hair. Indented sensory cells form the outer margin of the hair at this level. Smaller cells occupy the central regions of this tissue layer. The longitudinal section at the right includes only a fraction of the total lever tissue. From top to bottom the longitudinal section includes woody lever tissue, the podium region, and some leaf tissue. The arrow indicates the sensory layer where five indented cells are shown in longitudinal section.

When a finely localized stimulus was applied from point to point along the hair, starting at the lever end, the response was negligible until the driver was positioned at the level of the indented cells. These observations are consistent with the results of the destructive dissection experiments. All these data agree with the nineteenth century notion that the sensory cells should be located at the indentation of the hair where bending strains are relatively pronounced upon stimulation.

The cross-section of Fig. 3 indicates that there are several smaller cells located in the center of the rosette formed by the indented cells. None of our experiments excludes the possibility that these central cells are the primary sensory cells. However, the results of the intracellular measurements suggest that the central cells are an unlikely possibility. For the present, we assume that the indented cells of the sensory layer are the primary sensory cells.

Part 2. Intracellular Response of the Sensory Cells

Again sensory hairs were excised and mounted as shown in Fig. 1. In this case the proximal (upper) end of the hair was dissected away to the cell layer immediately above the indented level of the hair. This was an important preliminary to the intracellular probing because even very strong glass micropipettes would not penetrate a large number of plant cell walls. The exposed cell layer was immersed in perfusion fluid, and a glass micropipette probed through the tissue from above. Given the initial disadvantage of penetrating rigid cell walls, the preparation did have the subsequent advantage that the impaling micropipette was quite stable in the cell even when the preparation was deformed repeatedly by mechanical stimuli. The upper and lower chambers, separated by the insulation layer of the EM grid, each contained an Ag-AgCl electrode for monitoring the external response of the sensory cells. Either external electrode could be selected as a reference for the micropipette.

The potential measured by the micropipette changed abruptly relative to the potential of a reference electrode in the upper chamber when the probe penetrated a cell, and the potential returned to its original value when the probe was withdrawn from the cell. On the basis of the resting membrane potential, measured in the absence of a stimulus, the cells could be separated into two classes: (a) those which exhibited resting potentials of about −80 mv (−60 to −90 mv) and (b) those which exhibited resting potentials of about −30 mv (−20 to −40 mv). If the size of the cell could be estimated crudely by the distance which a micropipette had to be advanced after initial penetration but before the resting potential vanished again, resting potentials of −80 mv were associated with large cells and resting potentials of −30 mv were associated with small cells. The larger −80 mv cells were assumed to be the sensory cells since graded and all-or-none responses were recorded intracellularly when the preparation was stimulated. No measurable sensory re-

sponse to stimulation could be observed intracellularly for the smaller −30 mv cells, even though the external recording electrodes indicated that the gross extracellular response was normal for these preparations. These results suggest that the smaller, central cells behaved as a passive shunt path in the sensory layer, and the electrical properties of the central region of the sensory layer will be represented by passive resistance R_n in parallel with the indented sensory cells.

Typical intracellular response records are shown in Fig. 4. The upper trace was used to monitor the response recorded with extracellular electrodes, the second trace shows the response recorded with the intracellular micropipette referred to E_1, the third trace monitored stimulus force, and the fourth
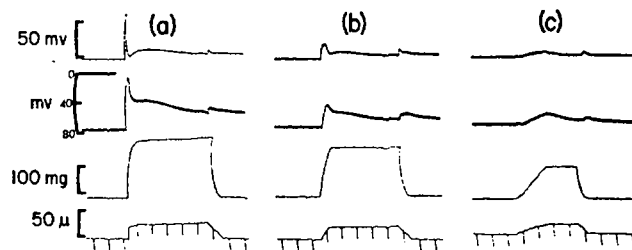

Figure 4. Response records from a typical preparation. Responses for three different stimulus conditions are shown in column a, b, and c. V_{ext} was recorded on the upper trace, the second trace monitored the response recorded with the intracellular micropipette referred to E_1, the third trace monitored stimulus force, and stimulus displacement was recorded on the fourth trace. Time marks separated by 1 sec were mixed with the displacement signal on the fourth trace. Positive potential differences shown upward, and the radius of curvature of the curvilinear recording system is indicated on the amplitude calibrations. The resting potential of the sensory cell was −80 mv ± 5 mv.

trace shows the position of the stimulus driver. Time marks separated by 1 sec were mixed with the signal of the position sensor on the fourth trace. The response recorded in column (a) of Fig. 4 was a maximal response in the sense that increasing stimulus force would not increase the amplitude of the response. This response includes a rapid depolarization phase of what has been termed the action potential. This was followed by a relatively rapid initial repolarization phase and then a slower repolarization phase. The stimulus remained on during the time of occurrence of the rapid repolarization phase of the response, and complete repolarization to the resting level did not occur immediately after the stimulus was switched off. A second depolarization, observed when the stimulus was switched off, may be a stimulus artifact. However, the stimulus monitors indicate that this is unlikely. While flexion of the micropipette tip might account for this stimulus off-effect in intracellular records, the off-effect was also observed routinely in the extracellular response which was measured with gross electrodes. The best guess at this time would

seem to be that the off-effect is biological in origin, either a function of the electrical response system of the sensory cells or a function of the mechanical properties of the cell walls. Graded responses are shown in columns (b) and (c) of Fig. 4. In column (b), the rate of rise and amplitude of the stimulus were less than for the records of column (a). Again there was a rapid depolarization phase and repolarization phase of the response. Notice, however, that the amplitude of the action potential was considerably less than for the earlier maximal response. In column (c) the rate of rise and amplitude of the stimulus were reduced further, the response did not show either a rapid phase of depolarization or a rapid phase of repolarization, and the response waveform more closely approximated the stimulus waveforms. The reference electrode for the recordings of Fig. 4 was positioned in the upper chamber for both intracellular and extracellular measurements. When the reference electrode was switched to the lower chamber, the sign of the response recorded by the extracellular electrodes reversed as expected while the sign of the intracellular response components was unchanged.

The sensitivity of preparations, as measured by the stimulus force required to elicit a particular response, varied from preparation to preparation. In general, hairs excised from more mature traps required greater force for a given amount of deformation. With the stiffer hairs, it was often more difficult to elicit a series of graded responses to graded stimuli than was the case for hairs excised from younger traps. The response characteristics also showed considerable variation from preparation to preparation, and the response characteristics frequently showed considerable variability for a given preparation when subjected to a series of control stimuli. While the records of Fig. 4 were selected to provide a representative sample of response waveforms, examples of extremes of variation are shown in Figs. 5 and 6. These variations were never observed in a single preparation, and the examples shown were selected from several preparations. The records of column (a) of Fig. 5 show a case in which the extracellular response exhibited a large negative phase which was
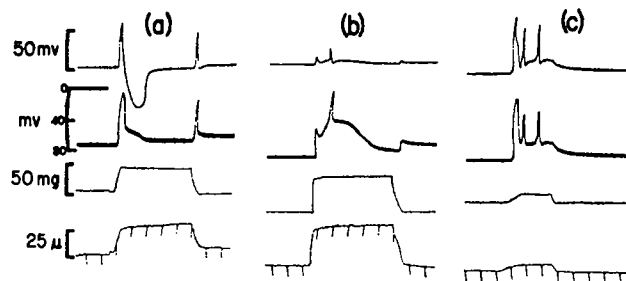

FIGURE 5.   Extreme response variations. Responses recorded from three different preparations are shown in columns a, b, and c. Details of the recording traces are identical to those of Fig. 4.

absent from the intracellular record. In column (b) the intracellular response exhibits a peculiar waveform, and notice that the extracellular response amplitude was considerably less than the magnitude of the intracellular response. Column (c) shows multiple rapid depolarizations in response to a single stimulus and there was no measurable off-response when the stimulus was turned off. In Fig. 6, the extracellular response shows an initial rapid depolarization phase which was not observed in the intracellular record; a second rapid depolarization phase was measured extracellularly which corresponds in time to the single rapid depolarization observed intracellularly. The records in Fig. 5 a and in Fig. 6 provide rarely observed examples in which the waveform of fast response components did not correspond in time for the extracellular and intracellular recordings. The much more typical observation of a one-to-
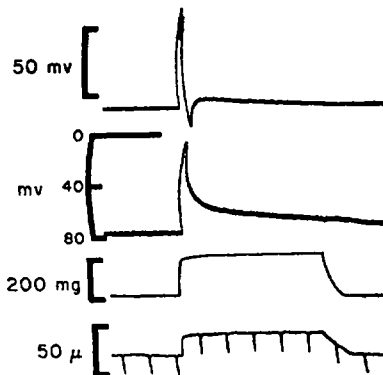

FIGURE 6. Unusual occurrence of asynchrony. Recording details for the four traces are identical to those of Fig. 4. Notice that the events recorded on the upper trace (V_{ext}) do not correspond in time to the events recorded on the second trace (V_{int}).

one correspondence between the complicated extracellular recordings and the intracellular recordings was a somewhat surprising result of these experiments.

The initial potential change of the response was always in a direction to depolarize the cell. An initial negative-going response was never observed intracellularly even when high velocity stimuli were applied to the preparation of Fig. 1. However, if the backup tool was removed from the preparation, high velocity stimuli elicited negative-going potential changes similar to the "negative receptor potentials" reported by Jacobson (1965) for the leaf preparation. (These negative receptor potentials were never observed to contribute an action potential to the closure sequence.) With the backup tool removed from the excised hair preparation, the hair bent sharply where the lever of the hair was held by beeswax on the supporting EM grid. Apparently the negative potential is generated when the woody structure of the lever is

strained, whereas deflection of the hair *in situ* produces bending in the podium region. We shall ignore the negative potential change because the negative response does not seem to be generated by the cells of the sensory region and because the negative response does not contribute to the closure sequence.

DISCUSSION

If the recording micropipette was located inside a primary sensory cell, the sign of the intracellular response should not change as the reference location was switched from the upper chamber at potential E_1 to the lower chamber at potential E_2 . Either reference location would be external to the active current generator, and the direction of the current vectors between the micropipette and the reference electrode would be the same for either reference location. The expected result was observed, but this result alone is not sufficient to establish the recording site of the micropipette as inside the sensory cell. The same result would be observed if the micropipette were outside the sensory cell but in a location where the directions of the current vectors were the same for both reference locations. The latter possibility seems very unlikely for this preparation. The current path between the two reference locations was parallel to the long axis of the sensory hair because the insulation of the EM grid isolated the two chambers from each other and because the waxy exterior surface of the hair limited radial components of the current. Given an external current path between chambers which is normal to the plane of the sensory layer and given a planar sensory layer with a total depth of one cell diameter, it seems difficult to construct a situation in which the current directions could be the same for the two reference locations if the micropipette were outside a sensory cell. We conclude that the intracellular responses were recorded with the micropipette inside a primary sensory cell.

The data indicate that the graded response and the action potential both occur in a single sensory cell. That is, the graded response does not seem to be a process of a sensory cell which in turn triggers some other cell type to initiate an action potential. The arguments supporting this conclusion are similar to the preceding ones which indicate that the intracellular response was recorded from the primary sensory cell. Once initiated in the sensory cell, the action potential propagates over the leaf. A possible mechanism for propagation is suggested by the electron micrographs of Scala et al.[1] which demonstrate plasmodesmata (intercellular channels connecting plant cells) in the cells of the sensory hair and the leaf tissue.

It seems clear now that the complicated waveform of the extracellular response results from an equally complicated intracellular response of single sensory cells. The complications of the gross extracellular response do not have

[1] Scala, J., D. W. Schwab, and E. D. Simmons. 1969. Personal communication.

to be explained in terms of a superposition of single-cell responses which are displaced in time relative to each other. Within experimental ability to resolve the question, the intracellular responses observed in one sensory cell of a preparation were the same as those observed when neighboring cells were impaled. Furthermore the extracellular measurements indicated that unit responses were, with rare exceptions, synchronized in time. The intracellular response of a single sensory cell could not be distinguished experimentally from the equivalent response which would be observed if the inside of all the sensory cells were connected together by a low-resistance, shorting path. However, it is not clear how the single cell responses are synchronized in the sensory layer. Perhaps the cells are electrically tight-coupled by the plasmodesmata, that is, perhaps the plasmodesmata provide a low-resistance pathway which connects the n sensory cells.

Fig. 7 is an electrical model of the excised hair preparation which includes the intracellular and extracellular recording situations. The isopotential volume inside the sensory cells is indicated by point S, point P is outside the upper membranes of the sensory cells, and point L is outside the lower membranes. Resistances r_S, r_P, and r_L represent equivalent resistance values for n identical sensory cells. The rationale for this simplification is that experimentally we cannot distinguish between the response of a single cell and the combined response of n cells. Resistances r_S and r_P are parameters of the upper membranes of the sensory cells, and r_s and r_L are resistance parameters of the lower membranes of the sensory cells. The batteries, V, specify the emf's for the upper and lower membranes. The parameters R_P and R_L represent access resistances to the sensory layer from the upper podium chamber and lower lever chamber, respectively.

The response processes of a sensory hair occur extremely slowly in time, and even the action potential may persist for a second. Unless the membrane capacitance C is larger by orders of magnitude than is usual for other biological tissue, voltage differences arising from capacitive displacement currents, $C\left(\dfrac{dV}{dt}\right)$ should be negligible for this preparation. Consequently, capacitive reactances will be ignored in calculating the equivalent impedance of the sensory layer. Let R_{LP} denote the equivalent impedance of the sensory layer as seen looking across the points L and P.

$$R_{LP} = \frac{r_S r_P}{(r_s + r_P)} + \frac{r_S r_L}{(r_s + r_L)} \tag{1}$$

The open-circuit voltage across the sensory layer is defined by

$$V_{LP} = E_L - E_P.$$

$$V_{LP} = (E_L - E_S) - (E_P - E_S) = \left(\frac{r_L}{r_s + r_L}\,V\right) - \left(\frac{r_P}{r_s + r_P}\,V\right) \tag{2}$$
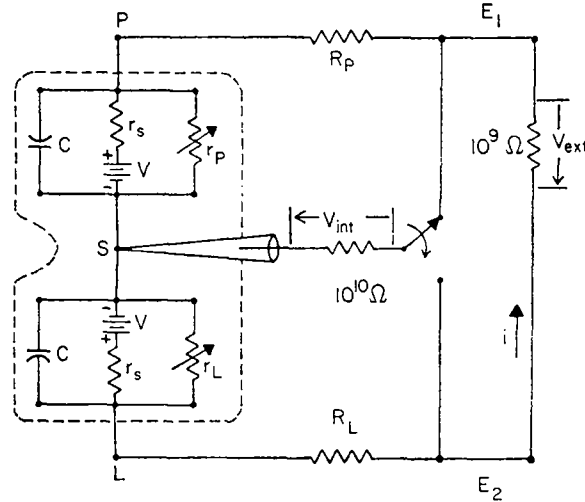
FIGURE 7. Electrical model of the excised hair preparation. The dashed line encloses the electrical components of the indented sensory layer. Point S represents the isopotential volume inside the sensory cells, P represents a point just outside the upper (podium) membranes of the sensory cells, L represents a point just outside the lower (lever) membranes of the sensory cells. V and r_s specify an emf and series resistance for the upper and lower membranes. The variable shunt resistance of the upper membranes is specified by r_P, and the corresponding variable parameter for the lower membrane is represented by r_L. Membrane capacitances are specified by C. R_P and R_L are access resistances to the sensory layer from the upper and lower external electrodes, respectively. The external current is specified by i. As for Fig. 1, E_1 is the potential of an external electrode in contact with the bathing solution in the upper (podium) chamber, E_2 is the potential of an external electrode in the lower (lever) chamber, $V_{ext} = (E_2 - E_1)$, and V_{int} is the difference in potential measured between a micropipette at point S and an external reference electrode. A fixed resistance R_n should be connected between points P and L of the model to represent the shunt path of the central region of the sensory layer. However, for convenience of analysis, R_n has been included as components of r_P and r_L. See text.

$$V_{LP} = \left[\frac{r_s(r_L - r_P)}{(r_s + r_L)(r_s + r_P)} \right] V \tag{3}$$

Equations (1) and (3) specify the impedance and voltage of the Thevenin generator which is equivalent electrically to the sensory layer. This voltage generator and its associated impedance R_{LP} are in series with the external impedances R_P, R_L, and $10^9\Omega$, and these define the current i.

$$i = \left[\frac{r_s(r_L - r_P)}{(r_s + r_L)(r_s + r_P)} \right] \frac{V}{R_{LP} + R_P + 10^9\Omega + R_L} \tag{4}$$

V_{ext} is simply the product (i) ($10^9\Omega$)

$$V_{ext} = E_2 - E_1 = \left[\frac{r_s(r_L - r_P)}{(r_s + r_L)(r_s + r_P)} \right] \frac{(V)(10^9\Omega)}{R_{LP} + R_P + 10^9\Omega + R_L} \tag{5}$$

If the input impedance of the external detector is much larger than the equivalent impedance of the rest of the circuit, the expression for V_{ext} simplifies. For $10^9 \Omega >> R_P + R_L + R_{LP}$

$$V_{ext} = \left[\frac{r_s(r_L - r_P)}{(r_s + r_L)(r_s + r_P)} \right] V \tag{6}$$

Notice that V_{ext} vanishes for electrical symmetry of the sensory layer. In the present model the condition of symmetry is that $r_L = r_P$, whence $V_{LP} = 0$, $i = 0$, and $V_{ext} = 0$ from equations (3), (4), and (6). In the absence of stimulation, the data indicate that V_{ext} approaches zero and the sensory layer approaches a symmetrical electrical configuration. But V_{ext} was nonzero during the response period, and during this period the electrical properties of the sensory layer cannot be symmetrical. These symmetry properties of the sensory layer are independent of our choice of model, because the equivalent electrical generator of the sensory layer, V_{LP}, would be zero for all symmetrical configurations and nonzero for asymmetrical configurations. Therefore if the destructive dissection experiments have been interpreted correctly, the upper membranes of a sensory cell behave differently from the lower membranes during the response period.

The expression for V_{ext} in equation (6) could be simplified considerably by assuming $r_P << r_s << r_L$. Although these conditions do not apply in general they seem to be approached in the limit at the positive peak of a maximal response. For this special case, equation (6) reduces to

$$\text{Lim } (V_{ext})_{max} = V \tag{7}$$

Given V_{ext} and a conservative potential field, we require only one intracellular potential difference measurement to uniquely define all the measurable potential differences shown for the model. The notation V_{int_1} will be used to specify the intracellular potential difference measured between the micropipette at potential E_s inside a sensory cell and a reference electrode at potential E_1.

$$V_{int_1} = E_s - E_1 = \frac{\dfrac{r_P}{r_P + r_s} (-V)}{\dfrac{r_s r_P}{r_s + r_P} + R_P + 10^{10}\Omega} \, 10^{10}\Omega \tag{8}$$

On the assumption that $10^{10}\Omega >> \dfrac{r_s r_P}{r_s + r_P} + R_P$

$$V_{int_1} = -\frac{r_P}{r_s + r_P} V \tag{9}$$

For completeness, we derive an explicit expression for V_{int_2}.

Again assuming $10^{10}\Omega >> \dfrac{r_s r_L}{r_s + r_L} + R_L$

$$V_{int_2} = E_S - E_2 = -\frac{r_L}{r_s + r_L} V \tag{10}$$

However, V_{int_2} is not an independent parameter of the system, since it can be expressed as the difference of two previously defined potential differences.

$$V_{int_2} = E_s - E_2 = (E_s - E_1) - (E_2 - E_1) = V_{int_1} - V_{ext} \tag{11}$$

As far as the electrical model and the data are concerned, it is arbitrary whether the variable parameters are r_P and r_L or whether two variable elements are substituted for the fixed values of r_s. However, r_P and r_L were chosen as the variable parameters on the speculative basis that response activity is probably associated with increased permeability of the sensory membranes. We now calculate limiting values for V, r_L, r_P, r_s, and R_n from typical data such as those of Fig. 4, given an estimated uncertainty of 5 mv for measuring potential differences in this experimental system.

The resting value of V_{int_1} was about -80 mv. When the preparation was stimulated, V_{int_1} changed in a positive direction, and the peak magnitude of the change was about 80 mv. Within resolution of the measurement, the cell depolarized completely at the response peak so that $V_{int_1} = 0$ mv.

On the hypothesis of the model, the magnitude of the emf of the sensory membrane must be at least as large as the resting value of V_{int_1}. Hence $| V | \geq$ 80 mv $\pm$ 5 mv. If $| V | = 80$ mv $\pm$ 5 mv, the data and equation (9) predict that $r_P \geq 10 \, r_s$ for the resting situation. When $V_{int_1} = 0 \pm 5$ mv at the peak of a maximal response, $r_P \leq \dfrac{r_s}{10}$. A recording of V_{int_2} was not shown explicitly in Fig. 4, but V_{int_2} is defined completely by the recordings of V_{int_1} and V_{ext} through the relation of equation (11). V_{int_2} was about -75 mv $\pm$ 5 mv in the resting state. Again on the assumption that $| V | = 80$ mv $\pm$ 5 mv, equation (10) predicts that $r_L \geq 10 r_s$ in the resting state. Upon stimulation, V_{int_2} changed by 15 mv $\pm$ 5 mv in a positive direction. Hence $V_{int_2} = -60$ mv $\pm$ 5 mv and from equation (10), $r_L \geq 3 r_s$ at the peak of the response. The value of r_P decreased by a factor of at least 100 as the sensory cell changed from the resting state to a peak response state, while the value of r_L decreased by at most a factor of 3 for the same state change.

As indicated earlier in the Results section, the central region of the sensory layer appears to behave as a passive shunt resistance. A fixed resistance R_n could have been connected between points P and L in Fig. 7 to represent this shunt path, but then the formal analysis of the model would have become

extremely cumbersome in notation. In order to calculate the magnitude of R_n, we now seek values for components of r_P and r_L which are equivalent electrically to R_n. The preceding formal analysis remains valid if both r_P and r_L are separated into two parallel resistances. Let r_P be the parallel combination of a variable resistance $\bar{r}_P$ which is solely a property of the upper sensory membranes and a second resistance which is the proper equivalent component of R_n. Let r_L be the parallel combination of a variable resistance $\bar{r}_L$ which is solely a property of the lower sensory membranes and another resistance which is the proper equivalent component of R_n. Values for the equivalent components of R_n can be calculated for several limiting cases. When $\bar{r}_P \to 0$ and $r_P \to 0$, the equivalent resistance in parallel with $\bar{r}_L$ must take the value R_n; r_L is defined by the parallel combination of $\bar{r}_L$ and R_n. When $\bar{r}_L \to 0$ and $r_L \to 0$, r_P is defined by the parallel combination of $\bar{r}_P$ and R_n. For the symmetrical case in which $\bar{r}_P = \bar{r}_L$ and $r_P = r_L$, r_L is defined by the parallel combination of $\bar{r}_L$ and $\frac{1}{2} R_n$, and r_P is defined by the parallel combination of $\bar{r}_P$ and $\frac{1}{2} R_n$. Since limiting values for r_P and r_L have already been derived from data such as those of Fig. 4, we can estimate a limiting value for the resistance R_n. For the symmetrical resting condition, $r_L \geq 10 \, r_S$. Both parallel components of r_L must satisfy this inequality individually; that is, $\bar{r}_L \geq 10 \, r_S$ and $\frac{1}{2} R_n \geq 10 \, r_S$. Therefore R_n is at least 20 times greater than the fixed resistance r_S. If R_n were neglected altogether in the analysis, steady-state parameters would change by no more than 10% as R_n was at least 10 times greater than $2 \, r_S$.

For freshly excised sensory hairs, the resting value of V_{ext} was about -10 mv. However, when the hair was stimulated repeatedly for a matter of hours, the resting value of V_{ext} slowly drifted in a positive direction to a value as large as $+5$ mv. Consequently, electrical symmetry of the resting preparation was defined within the limits $0.9 \leq \dfrac{\bar{r}_P}{\bar{r}_L} \leq 1.2$. The peak response asymmetry was typically defined by $\dfrac{\bar{r}_P}{\bar{r}_L} \leq 0.03$. The question remains as to how electrical asymmetry arises in an apparently symmetrical histological structure. On the assumptions (a) that the permeability changes of the sensory membranes are proportional to the deformation produced by mechanical stimuli and (b) that when deformed to the same extent the upper and lower membranes exhibit the same permeability changes, the response asymmetry would be observed if mechanical stimuli produced different deformations in the upper and lower membranes. Such deformation differences seem plausible because the upper membranes are adjacent to the relatively soft podium tissue, while the lower membranes are adjacent to the stiff woody structures of the lever tissue. These arguments would suggest that r_P should change more than r_L for a given stimulus, and this was the observed result. The fact that it was easier to grade re-

sponses for tender young hairs than for woodier mature hairs might also be explained by this type of argument.

Experimental results and equation (11) both predict that only two potential difference measurements are required to define V_{int_1}, V_{int_2}, and V_{ext}. As a practical matter V_{int_1} and V_{ext} provide the best experimental resolution with V_{int_2} a poor last choice. These practical considerations dictated the choice of displaying V_{int_1} and V_{ext} in Figs. 4–6. It is interesting to consider possible interpretations of the data given only one type of potential measurement. For example, if the only data available were those provided by V_{int_2}, the response asymmetry of the preparation would not have been apparent, and the peak amplitude of the response would have approached about 25% of that observed for V_{int_1}. If the only data available were those provided by V_{ext}, the response asymmetry would have been obvious, but V would only have been approximated through the limiting value of equation (7). V_{int_1} alone would have provided the best estimate of V, but again the response asymmetry would not have been obvious.

A more popular alternate to the model which has been proposed here would include ionic conductance parameters in series with specific Nernst batteries. The model of Fig. 7 would take the same general electrical form as this alternate possibility if $\bar{r}_P$ and $\bar{r}_L$ were constant with $g_s = 1/r_s$ as the variable conductance associated with the Nernst battery V. There are two cases for the alternate model depending upon whether the conductance of the sensory cells decreases or increases during the response period. If a single Nernst battery V is postulated for each membrane, the variable conductance of the upper membrane would have to decrease (not increase) 100-fold during the response period. For the second case in which conductance increases during the response, at least one additional Nernst battery would have to be postulated for the alternate model. Let V_j be the additional Nernst battery with its associated variable conductance g_j. At the peak of the response $V_{int_1} \rightarrow 0$, hence $V_j \rightarrow -(g_s/g_j)V$ where g_s and g_j are measured at the peak of the response and $|V| \geq 80$ mv ± 5 mv. Unless $V_j \rightarrow 0$, V_j must have a polarity opposite to V. If $V_j \rightarrow 0$, the additional Nerst system behaves like a variable shunt; that is, the alternate model becomes indistinguishable from the model in Fig. 7 with $g_j \rightarrow \dfrac{1}{r_P}$. Qualitatively similar arguments can be applied to the lower membrane for either case of the alternate hypothesis. At this time potassium appears to be the dominant charge carrier in this system with other ions of lesser importance (Jacobson, 1968). However, the ionic data are not sufficient to specify selective conductance systems. Perhaps future work will indicate that the model of Fig. 7 is too simple in detail, but a more structured model seems inappropriate until the data demand further complexity.

The amplitudes of the extracellular response recorded in the excised hair

preparation were larger on the average than those observed with the leaf preparation (Jacobson, 1965). Except for required amplitude scaling, however, the results seem to be qualitatively similar. Because of the correspondence between the extracellular response and the intracellular response, Jacobson's three-dimensional stimulus-response map should apply equally well to the intracellular response of a single sensory cell. Preliminary experimental results were consistent with this expectation.

BIBLIOGRAPHY

BENOLKEN, R. M., and S. L. JACOBSON. 1967. Origin of the sensory response in Venus' flytrap. Biophysical Society 11th Annual Meeting, Biophysical Society, New York. 47.

BROWN, W. H. 1916. The mechanism of movement and duration of the effect of stimulation in the leaves of Dionaea. *Amer. J. Bot.* **3:**68.

BROWN, W. H., and L. W. SHARP. 1910. The closing response in Dionaea. *Bot. Gaz.* **49:**290.

BURDON-SANDERSON, J. S. 1873. Note on the electrical phenomena which accompany stimulation of the leaf of Dionaea muscipula. *Phil. Trans. Roy Soc. London* **164:**495.

DiPALMA, J. R., R. MOHL, and W. BEST, JR. 1961. Action potential and contraction of Dionaea muscipula (Venus flytrap). *Science (Washington)*. **133:**878.

JACOBSON, S. L. 1965. Receptor response in Venus's fly-trap. *J. Gen. Physiol.* **49:**117.

JACOBSON, S. L. 1968. The ionic basis for the response to stimulation of Venus's fly-trap. Ph.D. dissertation, University of Minnesota.

MacNICHOL, E. F., JR., and H. G. WAGNER. 1954. A high impedance input circuit for electrophysiological recording from micropipette electrodes. Naval Medical Research Institute Report NM000 019.03.01. Bethesda, Md.

SIBAOKA, T. 1966. Action potential in plant organs. *Symp. Soc. Exp. Biol.* **20:**49.